Journal of Water Sustainability, Volume 8, Issue 3, September 2018, 99-110

Arsenic Removal from Aqueous Solution by Using Aluminum-Zirconium Bimetal Oxide: Adsorption Characteristics and Mechanisms

Kun Wu[1,*], Qinbin Huang[1], Xue Yang[2], Ting Liu[2]

[1]School of Environmental and Municipal Engineering, Xi'an University of Architecture and Technology, Xi'an, Shaanxi, 710055, China

[2]College of resources and environment, Northwest A&F University, Yangling, Shaanxi, 712100, China

ABSTRACT

The adsorption properties of arsenate (As(V)) were investigated by using aluminum-zirconium bimetal oxide (AZBO) as an adsorbent. The adsorption kinetic results illustrated that AZBO exhibited a fast adsorption rate towards As(V), and the equilibrium of As(V) adsorption could be achieved within 2 h. The kinetic data of As(V) adsorption could be well fitted by the pseudo-second-order model, thus indicating the occurrence of chemisorption. According to the adsorption isotherm results, the maximum amount of As(V) adsorbed onto AZBO at pH = 7.0 was determined to be 115.53 mg/g via the Langmuir isotherm model. Meanwhile, the Freundlich model was perfectly applicable to the equilibrium data, which also suggested that the removal of As(V) is a chemisorption process. The optimal performance for As(V) removal was achieved at pH = 6.0 approximately, and As(V) adsorption was depressed at alkali conditions (pH >7). The adsorption of As(V) was also inhibited in the presence of some anions, which can compete with arsenate for adsorption sites on the adsorbent surface. In addition, the spectroscopic analysis results of Fourier transform infrared spectroscopy and X-ray photoemission spectroscopy demonstrated that the removal mechanisms of As(V) primarily include the adhesion to surface hydroxyl groups and the ligand exchange with impregnated sulfate anions on the surface of AZBO.

Keywords: Arsenic; adsorption; aluminum oxide; zirconium oxide

1. INTRODUCTION

Arsenic (As) pollution in drinking water is an important issue in the world, which poses a serious threat to human health, especially in developing countries and rural areas (Hughes, 2002; Smedley and Kinniburgh, 2002). In order to provide feasible strategies to solve this problem, it is required to develop highly efficient, low-cost, and easy-to-handle methods to remove As from contaminated water. The adsorption process has many advantages over the other conventional techniques with respect to removing As in small-scale systems (Mohan and Pittman, 2007). Many kinds of materials were used as adsorbents to remove As from aqueous solution, and nano-sized metal oxides have attracted more and more attention due to their special characteristics (Lata and Samadder, 2016). In the past decade, many researchers focused on the development of novel metal-based adsorbents for improving As removal. Zhang et al. (2009) fabricated Fe-manganese (Mn) binary oxide (FMBO) and Fe-copper (Cu) binary oxide for As(V) removal, and the two Fe-based bimetal adsorbents could exhibit

*Corresponding to: tomlikeit@163.com

DOI: 10.11912/jws.2018.8.3.99-110

greater As(V) adsorption capacities than that of pure Fe hydroxide (FeOOH) (Zhang et al., 2013). Dou et al. (2011) and Chen et al. (2013) synthesized Fe-cerium (Ce) binary oxide to remove As(V) from water, and this adsorbent also exhibited a satisfactory performance for As(V) adsorption. Based on our previous studies, the doping of Mn oxides can remarkably improve the performance of Al oxides for the adsorption of both As(V) and As(III) (Liu et al., 2015; Wu et al., 2012). Hence, these bimetal oxides not only have the advantages of single oxides but also can significantly improve the adsorption capacity because of their synergistic effects. However, as far as we know, no research has been reported about the removal of As(V) by using aluminum-zirconium bimetal oxides (AZBO) as an adsorbent. In this study, we fabricated a novel material of Al-Zr bimetal oxide (AZBO) via the co-precipitation method and used it as an adsorbent to remove As(V) from aqueous solution. The adsorption characteristics were investigated via the kinetic and equilibrium experiments. In addition, the effects of solution pH and coexisting anions on As(V) adsorption were also studied. Furthermore, several surface characterization analyses were conducted to reveal the adsorption mechanisms for As(V) removal by AZBO.

2. MATERIALS AND METHODS

2.1 Materials and adsorbent preparation

Aluminum chloride ($AlCl_3$) and zirconium nitrate ($Zr(NO_3)_4$) were used for the adsorbent preparation. The As(V) stock solutions were prepared with sodium arsenate ($Na_3AsO_4 \cdot 12H_2O$). Sodium nitrate ($NaNO_3$) was used to fix a constant ionic strength (0.01 M $NaNO_3$) of solutions. Additionally, sodium hydroxide (NaOH) and hydrochloric acid (HCl) were used to adjust pH of solutions.

To prepare AZBO, 0.3 mol $AlCl_3$ and 0.1 mol $Zr(NO_3)_4$ were diluted and mixed in 400 mL deionized water. Subsequently, the solution pH was controlled between pH 5.0 and 6.0. After the solid-liquid mixture was stirred for another 2 hours (h), the precipitates that formed were filtered and rinsed with deionized water until no sulfate was detected in the washing water. After that, the precipitates were dried in the oven (90°C) for 12 h, crused, sieved and stored for use.

2.2 Batch experiments and analytical methods

For all the batch experiments, 0.015 g adsorbent was added into a series of 150 mL flasks containing 50 mL of As(V) solution, which were shaken in an orbit shaker at 170 rpm for 24 h at T = 25 ± 0.5°C. In the adsorption kinetic experiments, the initial concentration of As(V) was 0.1 mM (initial pH = 7.0). The samples were obtained at designed time intervals from different flasks and filtered with a 0.45 μm polycarbonate filter membrane. In the adsorption equilibrium experiments, the concentrations of As(V) ranged from 0.05 to 1.6 mM. NaOH and HNO_3 solutions were added as needed to maintain the solution pH to approximately 7.0. The samples were collected after 24 h of contact and filtered with 0.45-μm membranes. In the pH effect experiments, the solutions of 0.1 M HCl and 0.1 M NaOH were used for the preadjustment of initial solution pH ranging from 4.0 to 10.0 (initial As(V) = 7.5 mg/L). In addition, five kinds of anions (chloride, sulfate, carbonate, phosphate, and silicate; C_{anions} = 1, 10, and 100 mM) were used to investigate the effects of coexisting anions on As removal. To evaluate the cost-effectiveness of AZBO, the used adsorbent in the treatment of As solutions (C_0 = 7.5 mg/L, pH = 7.0) was separated by membrane filtration and added into a flask containing 50 mL of NaOH solution (0.1 M) with a dosage of 3.0 g/L. Then, the flask was shaken for 24 h to accomplish the As(V)

desorption process. After that, the residual solid powders were separated, freeze-dried, and stored for use in the next adsorption cycle.

Arsenic concentrations were determined using spectroscopy equipment (AF-610A, Beijing Ruili Analytical Instrument Co., Ltd., China) on the basis of hydride generation atomic fluorescence (HGAFS). In addition, a field emission scanning electron microscope combined with energy-dispersive X-ray spectroscopy (Quanta FEG 250, FEI Ltd., USA) was used to obtain its surface characteristics. FTIR spectra were obtained by using a Nicolet 5700 FTIR spectrophotometer (Nicolet Co., USA) with a transmission model. Samples containing 10 mg of the adsorbent were ground together with 250 mg of spectral grade potassium bromide (KBr) in an agate mortar. XPS data were collected by using an ESCA-lab-220i-XL spectrometer (Shimadzu, Japan) with monochromatic Al Kα radiation (1486.4 eV).

2.3 Theory

In order to investigate the potential rate-controlling step of the batch adsorption process, kinetic data were fitted with the pseudo-first-order and pseudo-second-order models, which are respectively presented as follows in Eqs.1-2 (Ho and Mckay, 1998, 1999):

$$q_t = q_e(1-e^{-K_{ad}t}) \tag{1}$$

$$t/q_t = t/q_e + 1/(kq_e^2) \tag{2}$$

where, t is the contact time of adsorption experiment (h); q_e (mg/g) and q_t (mg/g) are respectively the adsorption capacity at equilibrium and at any time t; K_{ad} (1/h) and k (g/(mg·h)) are the rate constants for the two models, respectively.

To provide the quantitative information for adsorption isotherms, these data were fitted by the Langmuir and Freundlich isotherm models, respectively (Eqs. 3-4) (Freundlich, 1906; Langmuir, 1918):

$$q_e = \frac{q_m b C_e}{1+bC_e} \tag{3}$$

$$q_e = K_F C_e^{\frac{1}{n}} \tag{4}$$

where C_e is the equilibrium concentration in the solution (mg/L), q_e is the equilibrium concentration in the solid adsorbent (mg/g), q_m is the maximum adsorption capacity (mg/g), K_F is a constant related to the adsorption capacity ($mg^{1-1/n}.L^{1/n}/g$), b is a constant related to the adsorption energy (L/g), and n is a constant related to the adsorption energy.

3. RESULTS AND DISCUSSIONS

According to the kinetic curve for As(V) adsorption (shown in Fig. 1), the adsorption equilibrium could be achieved within 2 h, and the adsorption amount (q_t) value of As(V) was only increased by 3.5% after 48 h of reaction. This result means that the adsorption rate of As(V) on AMBO is higher than most of other adsorbents (Lata and Samadder, 2016; Mohan and Pittman, 2007). For example, Glocheux et al. (2014) synthesized Al-oxide-coated 3D-organised mesoporous silica for the removal of As(V) from contaminated synthetic ground-water, and the adsorption equilibrium of As(V) could not be reached until 5 h of reaction. To provide more information, the kinetic data were fitted with the pseudo-first-order and pseudo-second-order models. Based on the parameters listed in Table 1, the pseudo-second-model provided a better application to the kinetic data, thus indicating the occurrence of chemisorption reaction (Sen and Sarzali, 2008).

Adsorption isotherms are essential to

evaluate the adsorptive performance of different adsorbents towards the same adsorbate. Fig. 2 demonstrates the isotherm curve for As(V) adsorption onto AZBO. It is clear that the adsorption amounts of As(V) increased with the elevated equilibrium concentrations, and the saturated adsorption amounts of As(V) on AZBO was much greater than that on pure Al oxides (Goldberg and Johnston, 2001). To obtain more quantitative information, these data were fitted by the Langmuir and Freundlich isotherm models. The maxium adsorption capacity of As(V) for AZBO was determined to be 115.53 mg/g via the Langmuir model (Table 2). Hence, the combination with Zr oxides can remarkably improve the performance of Al oxides for As(V) adsorption. Meanwhile, AZBO exhibited a greater adsorption capacity for As(V) than that of Fe-Zr binary oxides (Ren et al., 2011). It is noted that the isotherm data were perfectly described by the Freundlich model, which showed a better applicability than the Langmuir model. As the Freundlich isotherm model is an empirical equation corresponding to the multilayer adsorption onto heterogeneous surfaces, this result correborated the occurrence of chemisorption during the As(V) removal process.

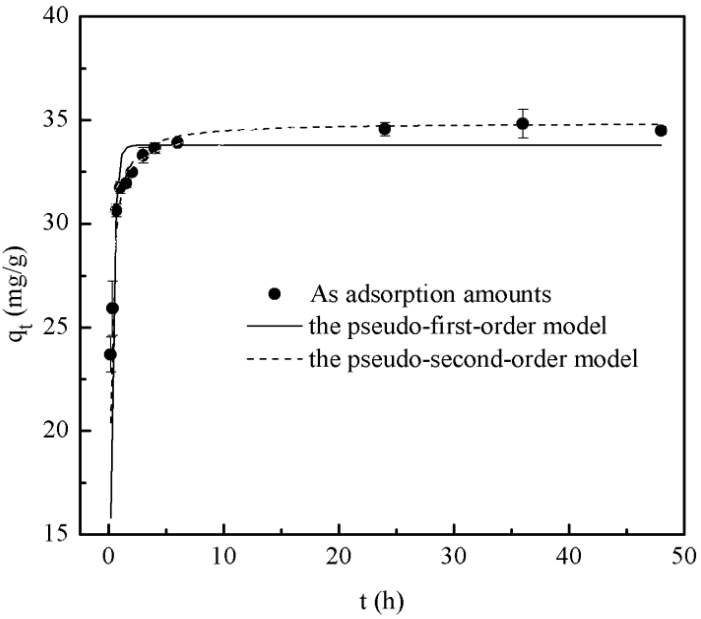

Figure 1 The kinetic curve of As(V) adsorption onto AZBO. Symbols indicate experimental data; solid lines represent the pseudo-first-order model; dash lines refer to the pseudo-second-order model. (Experimental conditions: initial As(V) = 7.5 mg/L, pH = 7.0, adsorbents dosage = 0.3 g/L, ion stength = 0.01 mM $NaNO_3$)

Table 1 Parameters of two kinetic models for the adsoption of As(V) onto AZBO

Kinetics models	**Parameters**		
Pseudo-first-order model	q_e (mg/g)	k_1 (1/h)	R^2
	33.78	3.78	0.815
Pseudo-second-order model	q_e (mg/g)	k_2 (g/(mg·h))	R^2
	34.89	8.457	0.98

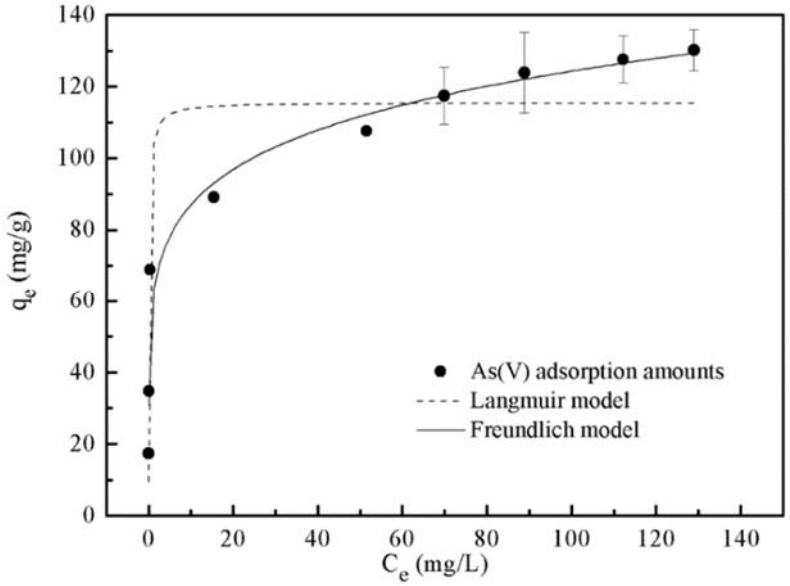

Figure 2 The isotherm curve of As(V) adsorption onto AZBO. Symbols indicate experimental data; solid lines represent the Freundlich model; dash lines refer to the Langmuir model. (Experimental conditions: initial As(V) = 3.75~120 mg/L, pH = 7.0, adsorbents dosage = 0.3 g/L, ion stength = 0.01 mM $NaNO_3$)

Table 2 Parameters of Langmuir and Freundlich isotherm models for fitting the isotherm data of As(V) adsorption onto AZBO

Isotherm models	**Parameters**	
Langmuir	q_e (mg/g)	115.53
	b (L/mg)	6.96
	R^2	0.900
Freundlich	K_f (g/(mg·L))	60.97
	1/n	0.155
	R^2	0.962

Solution pH is a key water quality factor affecting the adsorption performances of various adsorbates. As shown in Fig. 3, the adsorption amount of As(V) was initially increased from pH 4.0 and then reached a peak value at pH 6.0. When the solution pH was further increased from 6.0 to 10.0, the As(V) adsorption amount was decreased significantly. Hence, the pH range of 5.0~6.0 was suggested for the optimal removal of As(V) by AZBO. Han et al. (2013) used Al_2O_3 for the adsorption of As(V) and found the removal efficiency of As(V) remained constant in the pH range of 4.0~5.0 and then decreased in the pH range of 5.0~10.0, respectively. This phenomenon was attributed to the deprotonated reactions at high pH conditions, which would bring side effects on the ion exchange between $HAsO^{2-}/H_2AsO_4^-$ and OH^- (Han et al., 2013). This explanation can also apply well to the pH dependence of As(V) removal by AZBO. Moreover, when the pH was increased from 6.0 to 10.0, more OH^- competed with $HAsO^{2-}/H_2AsO_4^-$ in binding at the active sites on the surface of AZBO. This phenomenon could also account for the depressed As(V) adsorption at a higher pH.

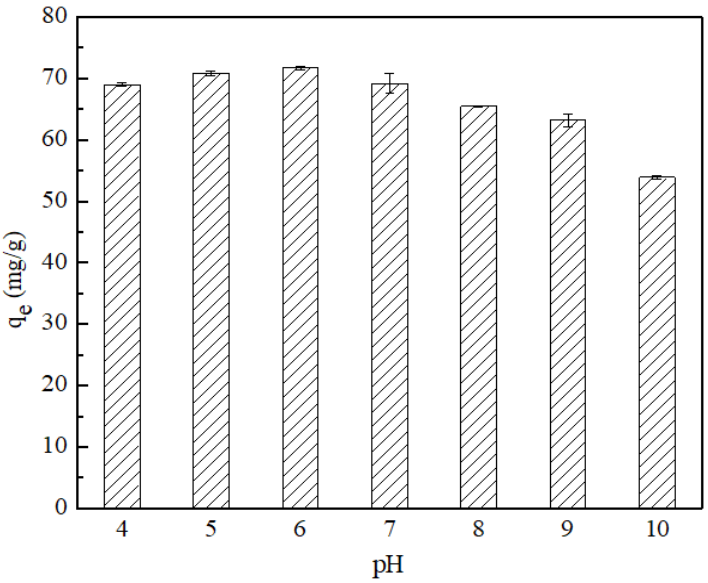

Figure 3 The effects of solution pH on the removal of As(V) by AZBO. (Experimental conditions: initial As(V) = 7.5 mg/L, pH = 4.0~10.0, adsorbents dosage = 0.3 g/L, ion stength = 0.01 mM $NaNO_3$)

Considering the complexity of practical contaminated waters, there is a need to investigate the influence of coexisting anions on As(V) adsorption. Fig. 4 shows the variations in adsorption amounts of As(V) with the coexistence of five different anions. It can be seen that the As(V) adsorption amounts were almost unchanged with the presence of chloride ions and sulfate. However, an evident decrease in the As(V) uptake was caused by the existence of carbonate, silicate, and phosphate, especially the phosphate anions. The side effects of these oxyacid anions on As(V) adsorption were mainly ascribed to the competition for the actives sites on the surfaces of Al oxides and Zr oxides. Because the elements of As and phosphorus (P) are located in the same main group and have a similar molecular structure, the competition effects between arsenate and phosphate are extremely intensive and thus significantly inhibiting the removal of As(V) (Qi et al., 2015).

To further investigate the mechanisms of As(V) adsorption onto AZBO, FTIR analysis was carried out using the pristine and As(V)-loaded samples. As shown in Fig. 5, a sharp peak at 1639.6/cm and a broad band centered at 3423.6/cm for the spectrum of the pristine AZBO were assigned to the adsorbed water or water hydration within the sample (Zhang et al., 2005). For pristine AZBO, the peak at 1128.5/cm was ascribed to the bending vibration of hydroxyl groups on the adsorbent surface (Asencios and Sun-Kou, 2012). These peaks were similar to that in the FTIR spectra of aluminum hydroxides (Asencios and Sun-Kou, 2012). In addition, the peaks at 613.7/cm was associated with S-O, which indicated that sulfate (SO_4^{2-}) anions were impregated into AZBO surface during the adsorbent preparation process (Peak et al., 1999; Zalkind et al., 2004). After the adsorption of As(V), the bands at 3423.6 and 1639.6/cm showed an unnoticeable shift. However, the peak at 1129/cm was shifted to 1124.1/cm, and an obvious decrease in its intensity could be observed. The shape change of the peaks for Al-OH indicated that As(V) anions might be bonded to the hydroxyl groups on AZBO surface. Moreover, there was a new

band centered at 861.3/cm, which was attributed to the stretching vibration of As-Obands in arsenate (Nero et al., 2010), appeared in the spectrum of the As(V)-reacted sample. Thus, it is confirmed that the As(V) anions were successfully adsorbed onto the surfaces of AZBO. Meanwhile, the peak at 613.7/cm was shifted to 614.3/cm and its intensity decreased significantly, which indicated the occurence of the ligand exchange between As(V) and sulfate in the reaction process.

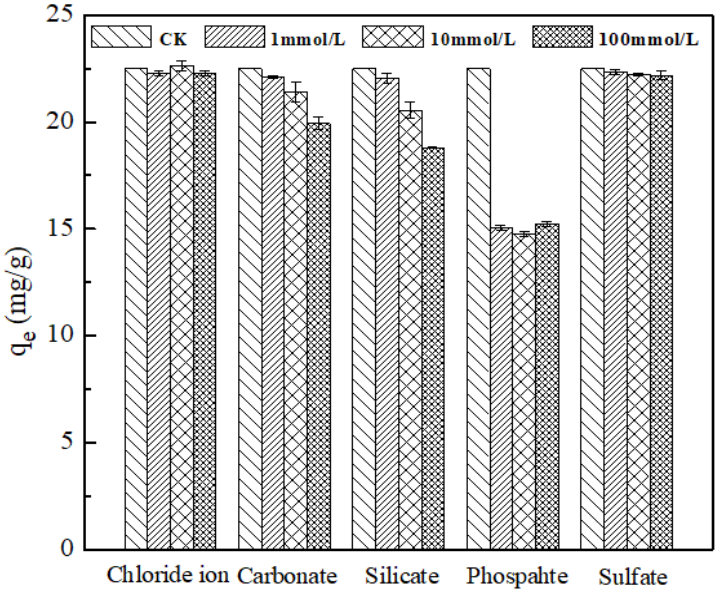

Figure 4 The effects of coexisting anions on the removal of As(V) by AZBO. (Experimental conditions: initial As(V) = 7.5 mg/L, pH = 7.0, adsorbents dosage = 0.3 g/L, ion stength = 0.01 mM $NaNO_3$)

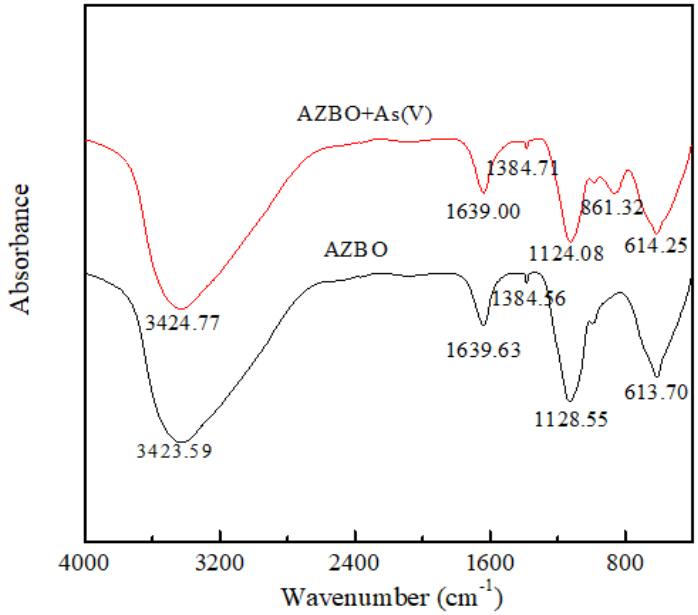

Figure 5 The FTIR spectra of AZBO before and after As(V) adsorption. (Experimental conditions: initial As(V) = 7.5 mg/L, pH = 7.0, adsorbents dosage = 0.3 g/L, ion stength = 0.01 mM $NaNO_3$)

To further explore the mechanisms of As(V) adsorption, XPS analysis was also conducted. The XPS all-scan spectra for the pristine and and As(V)-reacted samples were illustrated in Fig. 6. The peaks assigned to the elements of O, Al, Mn, and S could be clearly observed in the two curves. A new peak appeared in the spectrum of As(V)-reacted sample, which was in accordance with the capture of As(V). The O1s XPS spectra of samples before and after As(V) adsorption are illustrated in Fig. 7a and 7b, respectively. In Fig. 7a, the O1s spectrum for the pristine AZBO was divided into four peaks at 533.5, 530.9, 532.5, and 531.9 eV, which were corresponded to the loosely bounded oxygen of H_2O, the lattice oxygen within the metal oxides (Me-O), the hydroxyl oxygen within the hydroxyl groups (Me-OH), and the sulfur oxygen within the sulfate, respectively (Baltrusaitis et al., 2007; Biswas et al., 2006; Milanova et al., 2009; Wagata et al., 2011). The area ratio of Me-OH was 40.04%, which indicated that a plenty of hydroxyl groups existed on the surface of prisitine AZBO. After the adsorption of As(V), a new peak appeared at 532.4 eV (Fig. 7b), which was corresponded to As-O and had an area ratio of 31.7% (Ishikawa and Ikoma, 1992). Moreover, the area ratio for Me-OH was reduced to 18.8%, whereas a slight decrease was observed (from 17.79% to 16.77%) in the area ratio of Me-O (Fig. 6). The decrease in Me-OH intensity implied that the hydroxyl groups on AZBO surface played an importent role in the adsorption of As(V). Meanwhile, the reduced area ratio of S-O (from 37.64% to 17.28%) after the adsorption of As(V) indicated the ligand exchange between sulfate and As(V). Ma et al. (2011) used Zr-based nanomaterials for the adsorption of As(V), and they also found that the introduced sulfate into the adsorbent was involved in the reactions with arsenic at the solid-liquid interface. Therefore, the adsorption mechanisms for As(V) removal mainly include surface complexation and ligand exchange.

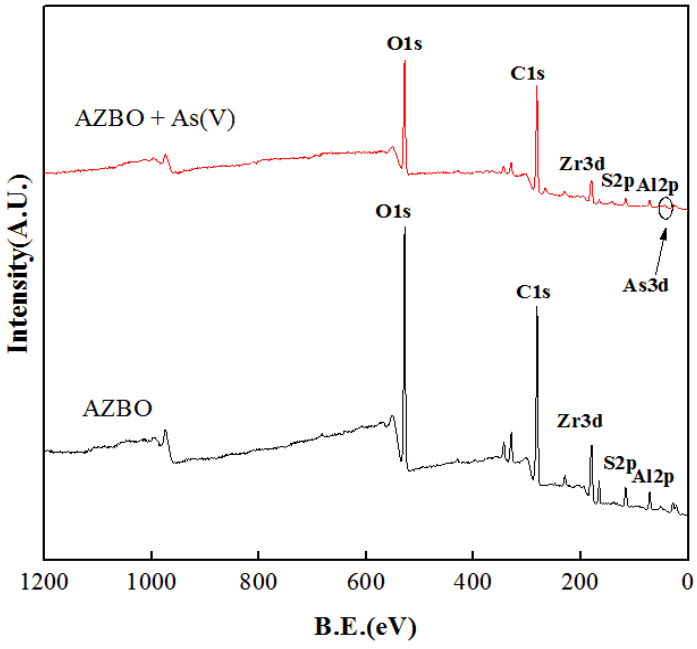

Figure 6 The XPS all-scan spectra of AZBO before and after As(V) adsorption. (Experimental conditions: initial As(V) = 7.5 mg/L, pH = 7.0, adsorbents dosage = 0.3 g/L, ion stength = 0.01 mM $NaNO_3$)

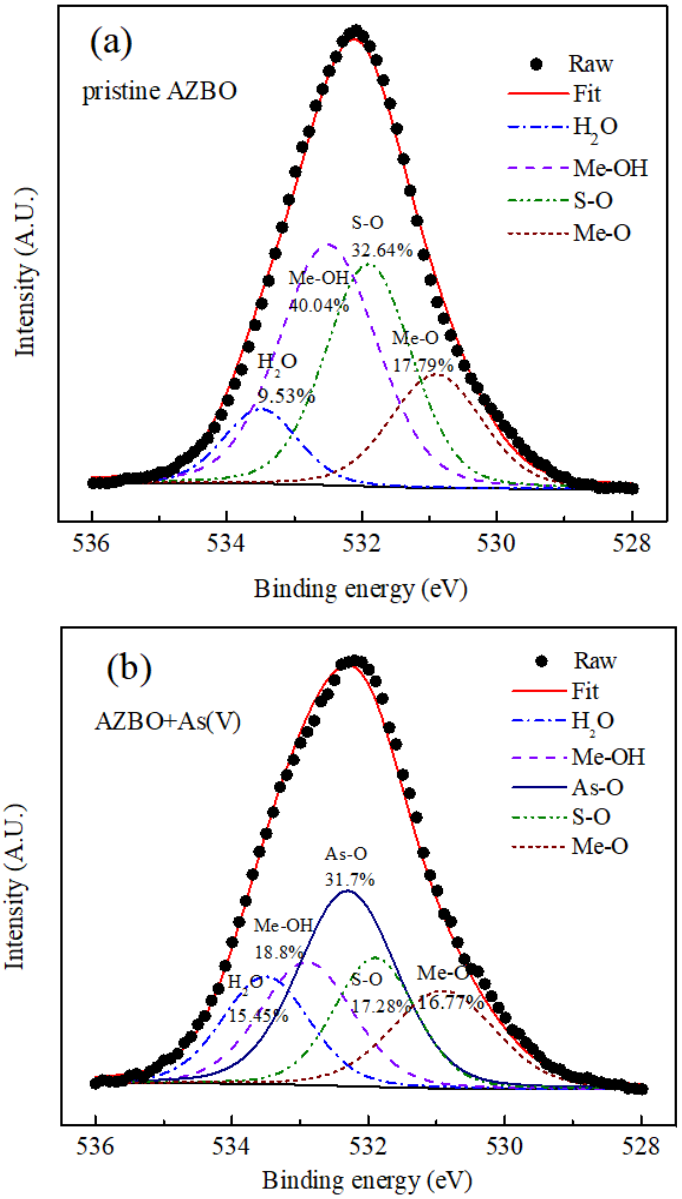

Figure 7 The O1s XPS spectra of AZBO before and after As(V) adsorption. (Experimental conditions: initial As(V) = 7.5 mg/L, pH = 7.0, adsorbents dosage = 0.3 g/L, ion stength = 0.01 mM $NaNO_3$)

To assess the reuse performance of this adsorbent, regeneration and reuse experiments were conducted using saturated AMBO for four consecutive cycles. Fig. 8 shows that the As amounts adsorbed onto AZBO decreased from 24.83 mg/g to 23.46 mg/g in the 1st and 4th time for use, which means that 94.5% of the original adsorption capacity of this adsorbent could be maintained after being used for four times. Hence, the regeneration & reuse results indicated that AZBO is renewable adsorbent to remove As(V) from contaminated water.

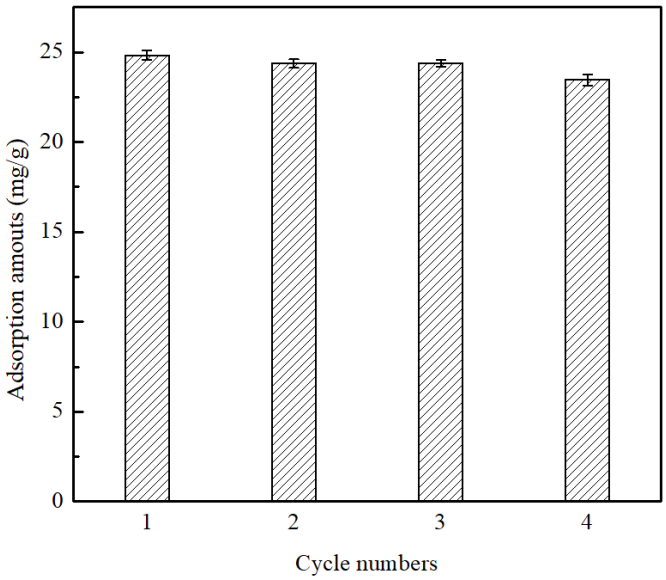

Figure 8 The performance of AZBO for the adsorption of As(V) in four consecutive adsorption-desorption cycles. (Experimental conditions: initial As(V) = 7.5 mg/L, pH = 7.0, adsorbents dosage = 0.3 g/L, NaOH = 0.1 mM, ion stength = 0.01 mM $NaNO_3$)

CONCLUSIONS

This research demonstrates that Al-Zr bimetal oxide can be used as a promising adsorbent for the removal of As(V) from aqueous solutions. AZBO not only has a fast rate for As(V) adsorption, but also exhibits a remarkable adsorption capacity. The kinetic data and the isotherm data were fitted well with the pseudo-second-order model and the Freundlich model, respectively. Compared with a majority of other composite adsorbents, AZBO exhibits a larger maximum adsorption amount (115.53 mg/g). The optimum pH range for As(V) removal was approximately 5.0~6.0, and the adsorption of As(V) was depressed at alkali conditions (pH >7). In addition, phosphate or silicate anions can bring noticeable side effects on As(V) adsorption through competition mechanisms. Furthermore, the results of FTIR and XPS indicated that the mechanisms of As(V) adsorption onto AZBO can be primarily attributed to the affinity with surface hydroxyl groups and the ligand exchange with the doped sulfate.

ACKNOWLEDGEMENTS

This work was supported by the Natural Science Foundation of China (Grant No. 51578440 / 51208415), the Science and technology overall plan of Shaanxi Province (No. 2016KTCG01-17), Key Laboratory Project of Education Department of Shaanxi Province (Grant No. 14JS042), and Major Science and Technology Program for Water Pollution Control and Treatment (Grant No. 2013ZX07310-001).

REFERENCES

Asencios, Y.J.O. and Sun-Kou, M.R. (2012). Synthesis of high-surface-areag-Al_2O_3 from aluminum scrap and its use for the adsorption of metals: Pb(II), Cd(II) and Zn(II). *Applied Surface Science*, 258(24), 10002-10011.

Baltrusaitis, J., Cwiertny, D.M. and Grassian, V.H. (2007). Adsorption of sulfur dioxide on hematite

and goethite particle surfaces. *Physical Chemistry Chemical Physics*, 9(4), 5542-5554.

Biswas, P.K., De, A., Dua, L.K. and Chkoda, L. (2006). Work function of sol-gel indium tin oxide (ITO) films on glass. *Applied Surface Science*, 253(4), 1953-1959.

Chen, B., Zhu, Z.L., Guo, Y.W., Qiu, Y.L. and Zhao, J.F. (2013). Facile synthesis of mesoporous Ce-Fe bimetal oxide and its enhanced adsorption of arsenate from aqueous solutions. *Journal of Colloid and Interface Science*, 398(15), 142-151.

Dou, X.M., Zhang, Y., Zhao, B., Wu, X.M., Wu, Z.Y. and Yang, M. (2011). Arsenate adsorption on an Fe-Ce bimetal oxide adsorbent: EXAFS study and surface complexation modeling. *Colloids and Surfaces A: Physicochemical and Engineering Aspects*, 379(1-3), 109-115.

Freundlich, H.M.F. (1906). Ünber die adsorption in lösungen. *Zeitschrift Fã¼r Physikalische Chemie*, 57U(1), 385-470.

Glocheux, Y., Albadarin, A.B., Galán, J., Oyedoh, E., Mangwandi, C., Gérente, C., Allen, S.J. and Walker, G.M. (2014). Adsorption study using optimised 3D organised mesoporous silica coated with Fe and Al oxides for specific As(III) and As(V) removal from contaminated synthetic groundwater. *Microporous and Mesoporous Materials*, 198(18), 101-114.

Goldberg, S. and Johnston, C.T. (2001). Mechanisms of arsenic adsorption on amorphous oxides evaluated using macroscopic measurements, vibrational spectroscopy, and surface complexation modeling. *Journal of Colloid and Interface Science*, 234(1), 204-216.

Han, C.Y., Pu, H.P., Li, H.Y., Deng, L., Huang, S., He, S.F. and Luo, Y.M. (2013). The optimization of As(V) removal over mesoporous alumina by using response surface methodology and adsorption mechanism. *Journal of Hazardous Materials*, 254-255(1), 301-309.

Ho, Y.S. and Mckay, G. (1998). Sorption of dye from aqueous solution by peat. *Chemical Engineering Journal*, 70(2), 115-124.

Ho, Y.S. and Mckay, G. (1999). Pseudo-second order model for sorption processes. *Process Biochemistry*, 34(5), 451-465.

Hughes, M.F. (2002). Arsenic toxicity and potential mechanisms of action. *Toxicology Letters*, 133(1), 1-16.

Ishikawa, T. and Ikoma, H. (1992). X-ray photoelectron spectroscopic analysis of the oxide of GaAs. *Japanese Journal of Applied Physics*, 31(Part 1, No. 12A), 3981-3987.

Langmuir, I. (1918). The adsorption of gases on plane surfaces of glass, mica and platinum. *Journal of the American Chemical Society*, 40(9), 1361-1403.

Lata, S. and Samadder, S.R. (2016). Removal of arsenic from water using nano adsorbents and challenges: a review. *Journal of Environmental Management*, 166, 387-406.

Liu, T., Wu, K., Xue, W. and Ma, C. (2015). Characteristics and mechanisms of arsenate adsorption onto manganese oxide-doped aluminum oxide. *Environmental Progress and Sustainable Energy*, 34(4), 1009-1018.

Ma, Y., Zheng, Y.M. and Chen, J.P. (2011). A zirconium based nanoparticle for significantly enhanced adsorption of arsenate: Synthesis, characterization and performance. *Journal of Colloid & Interface Science*, 354(2), 785-792.

Milanova, M., Iordanova, R. and Kostov, K.L. (2009). Glass formation in the MoO_3-CuO-PbO system. *Journal of Non-Crystalline Solids*, 355(6), 379-385.

Mohan, D. and Pittman, C.U.Jr. (2007). Arsenic removal from water/wastewater using adsorbents-a critical review. *Journal of Hazardous Materials*, 142(1-2), 1-53.

Nero, M.D., Galindo, C., Barillon, R., Halter, E. and Madè, B. (2010). Surface reactivity of α-Al_2O_3 and mechanisms of phosphate sorption: In situ ATR-FTIR spectroscopy and ζ potential studies. *Journal of Colloid and Interface Science*, 342(2), 437-444.

Peak, D., Ford, R.G. and Sparks, D.L. (1999). An

in situ ATR-FTIR investigation of sulfate bonding mechanisms on goethite. *Journal of Colloid and Interface Science*, 218(1), 289-299.

Qi, J.Y., Zhang, G.S. and Li, H.N. (2015). Efficient removal of arsenic from water using a granular adsorbent: Fe-Mn binary oxide impregnated chitosan bead. *Bioresource Technology*, 193, 243-249.

Ren, Z.M., Zhang, G.S. and Chen J.P. (2011). Adsorptive removal of arsenic from water by an iron-zirconium binary oxide adsorbent. *Journal of Colloid and Interface Science*, 358(1), 230-237.

Sen, T.K. and Sarzali, M.V. (2008). Removal of cadmium metalion (Cd^{2+}) from its aqueous solution by aluminum oxide (Al_2O_3): a kinetic and equilibrium study. *Chemical Engineering Journal*, 142(2), 256-262.

Smedley, P.L. and Kinniburgh, D.G. (2002). A review of source, behaviors and distribution of arsenic in natural waters. *Applied Geochemistry*, 17(5), 517-568.

Wagata, H., Ohashi, N., Katsumata, K.I., Okada, K. and Matsushita, N. (2011). The Effect of Citric Ion on the Spin-Sprayed ZnO Films: IR and XPS Study for the Organic Impurities. *Key Engineering Materials*, 485(485), 291-294.

Wu, K., Liu, T., Xue, W. and Wang, X.C. (2012). Arsenic(III) oxidation/adsorption behaviors on a new bimetal adsorbent of Mn-oxide-doped Al oxide. *Chemical Engineering Journal*, 192(2), 343-349.

Zalkind, O.A., Makarov, D.V. and Makarov, V.N. (2004). Determination of sulfate groups in complex mixtures by infrared spectroscopy. *Journal of Analytical Chemistry*, 59(8), 722-724.

Zhang, G.S., Liu, H.J., Liu, R.P. and Qu, J.H. (2009). Adsorption behavior and mechanism of arsenate at Fe-Mn binary oxide/water interface. *Journal of Hazardous Materials*, 168(2), 820-825.

Zhang, G.S., Ren, Z.M., Zhang, X.W. and Chen, J.P. (2013). Nanostructured iron(III)-copper(II) binary oxide: A novel adsorbent for enhanced arsenic removal from aqueous solutions. *Water Research*, 47(12), 4022-4031.

Zhang, Y., Yang, M., Dou, X., He, H. and Wang, D. (2005). Arsenate adsorption on an Fe-Ce bimetal oxide adsorbent: Role of surface properties. *Environmental Science and Technology*, 39(18), 7246-7253.